Spin-crossover Hofmann Frameworks Incorporating an Amide-functionalized Ligand: N-(pyridin-4-yl)benzamide

Xandria Ong[1], Manan Ahmed[1], Luonan Xu[1], Ashley T. Brennan[1], Carol Hua[2], Katrina A. Zenere[3], Zixi Xie[3], Cameron J. Kepert,[3] Benjamin J. Powell[4] and Suzanne M. Neville[1,*]

S1. Thermogravimetric analysis

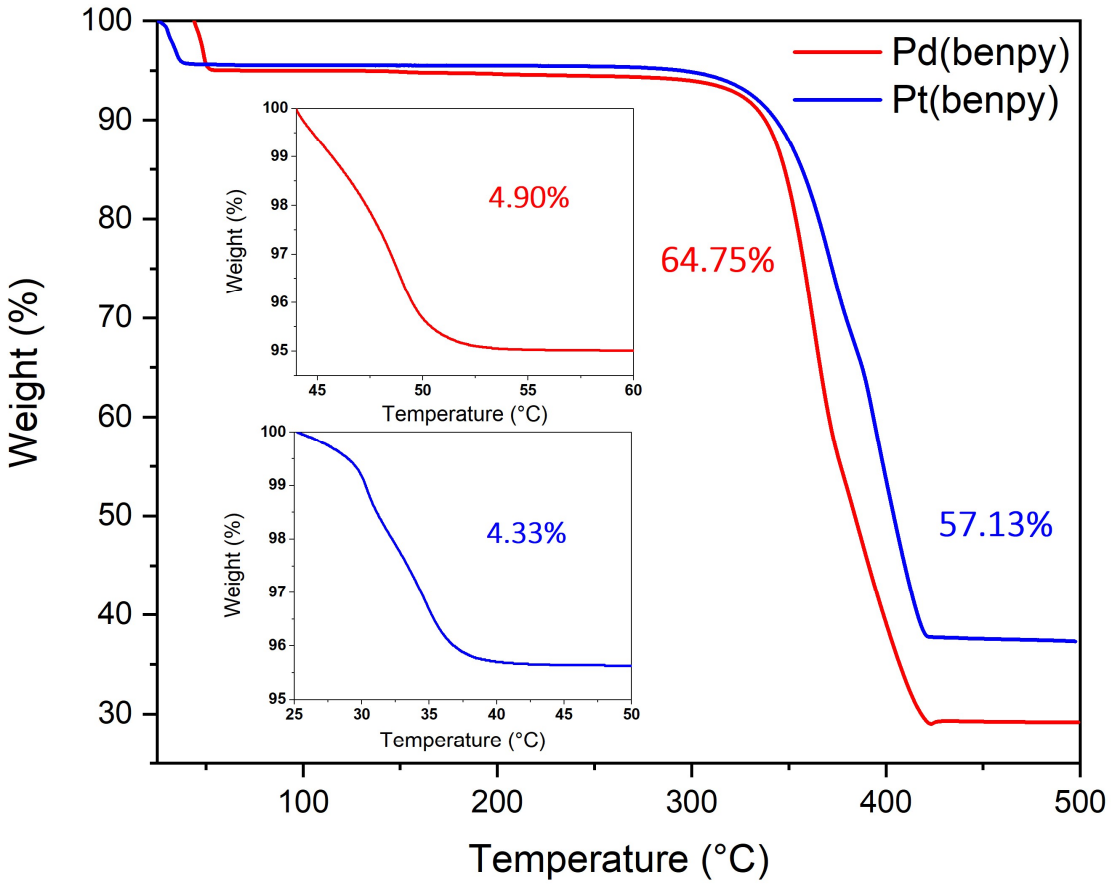

Figure S1. TGA data for **Pd(benpy)** (red) and **Pt(benpy)** (blue).

S2. Magnetic Susceptibility

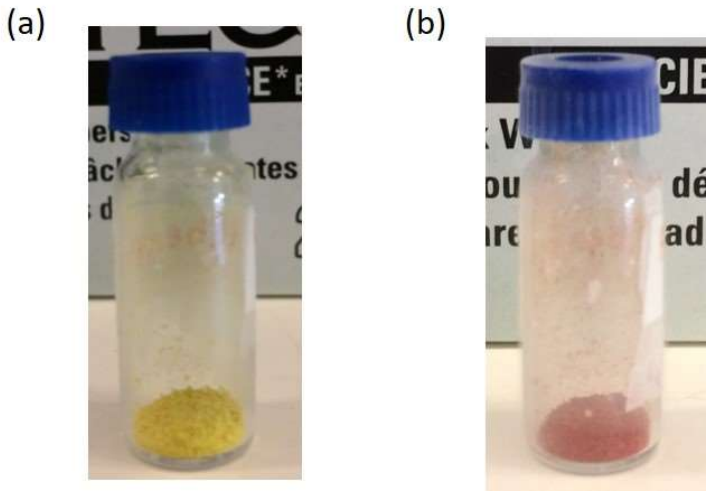

Figure S2. Example photo of **Pd(benpy)** and **Pt(benpy)** at (a) room temperature and (b) cooled in liquid nitrogen.

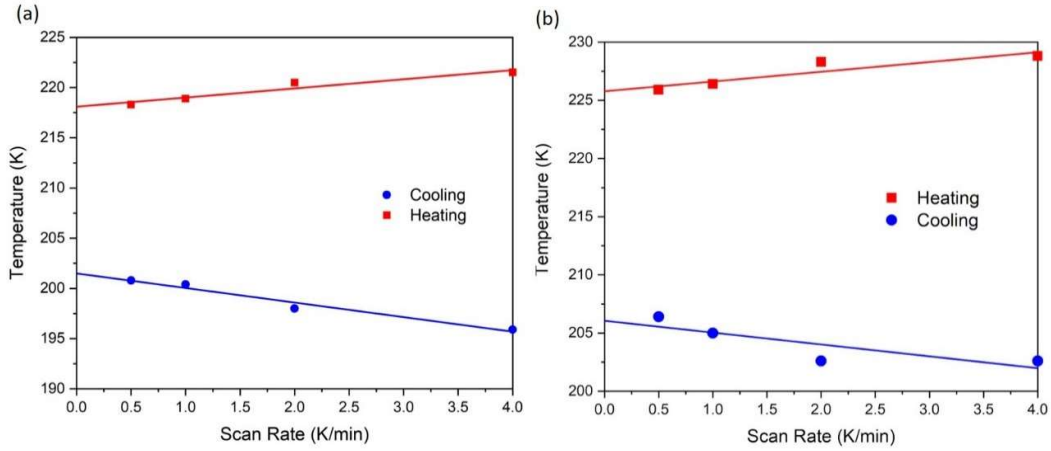

Figure S3. Plot of the scan rate versus transition temperature for (a) **Pd(benpy)** and (b) **Pt(benpy)**, extrapolated from Figures 2(a) & (b) of the manuscript.

S3. Magnetic susceptibility simulation

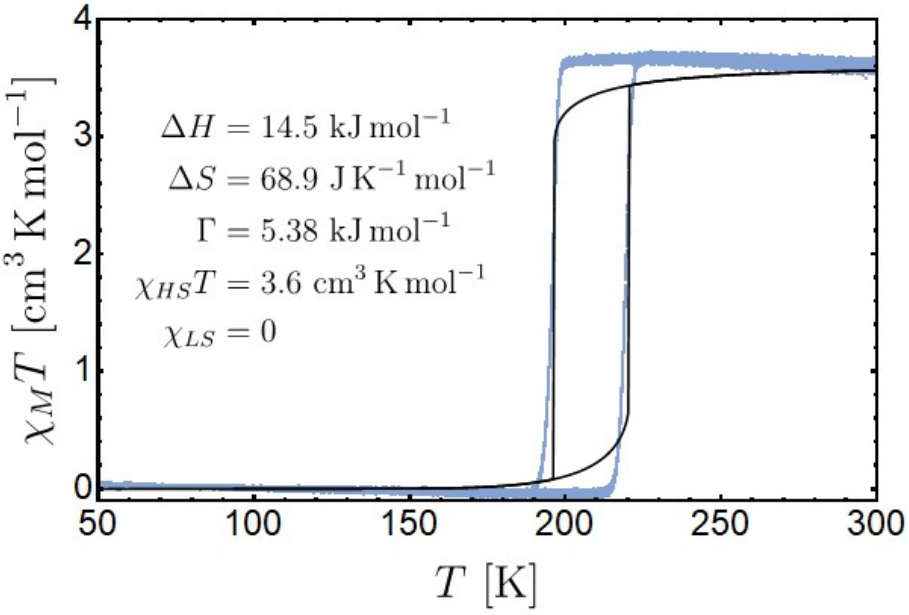

Figure S4. Plot of the simulated magnetic susceptibility for **Pd(benpy)** extrapolated from Figure 2(a) of the manuscript (2 $\mathrm{Kmin^{-1}}$ scan rate).

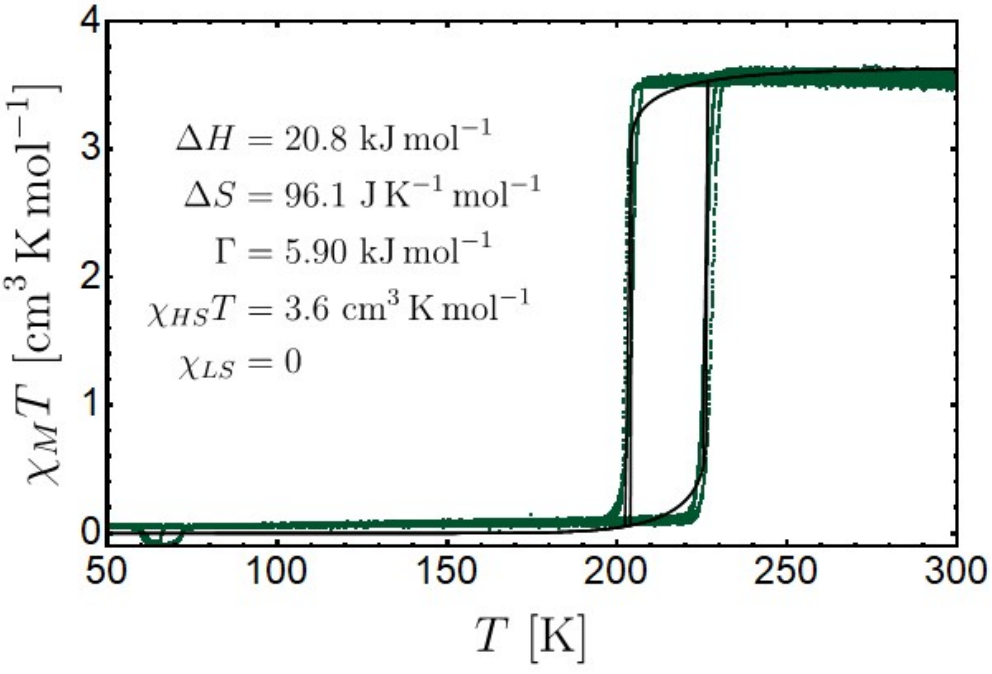

Figure S5. Plot of the simulated magnetic susceptibility for **Pt(benpy)** extrapolated from Figure 2(a) of the manuscript (2 $\mathrm{Kmin^{-1}}$ scan rate).

S4. Variable Temperature Powder X-ray Diffraction

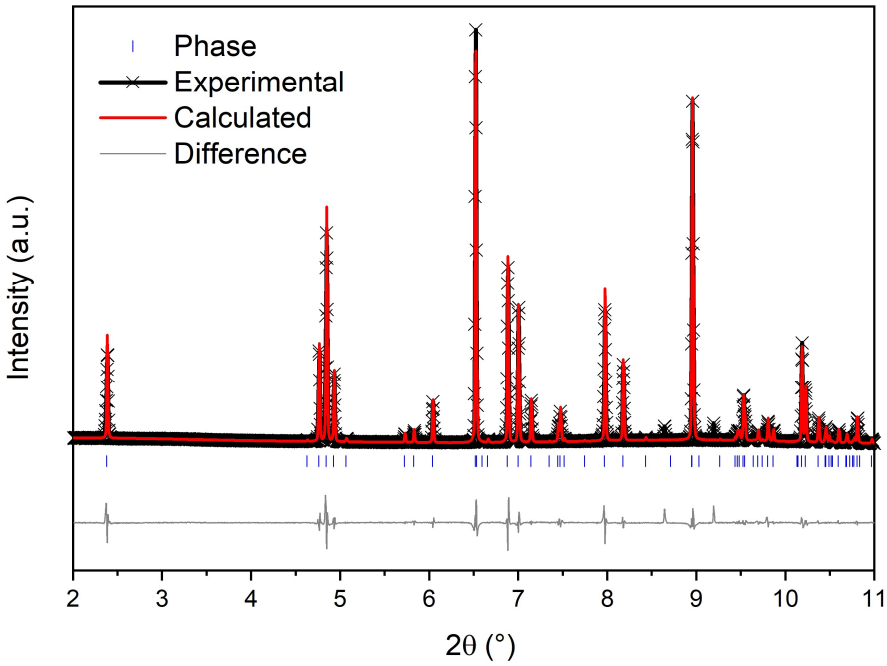

Figure S6. Le Bail fit of PXRD data for **Pd(benpy)** at 250 K. Refined parameters: a = 7.14 Å, b = 7.55 Å, c = 28.43 Å, β = 92.16°, V = 1531.86 Å^3.

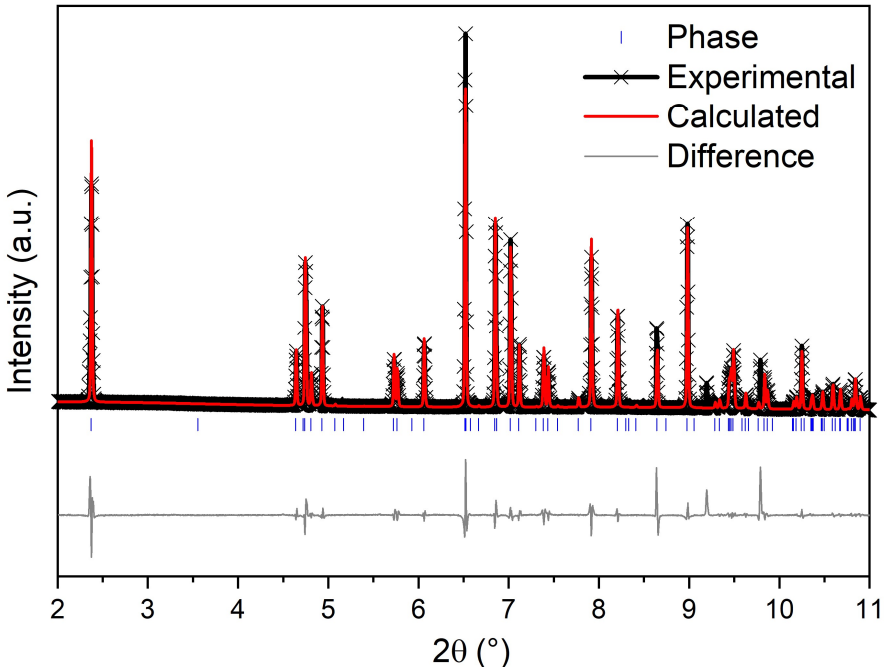

Figure S7. Le Bail fit of PXRD data for **Pt(benpy)** at 250 K. Refined parameters: a = 28.57 Å, b = 7.53 Å, c = 7.17 Å, β = 93.05°, V = 1541.37 Å^3.

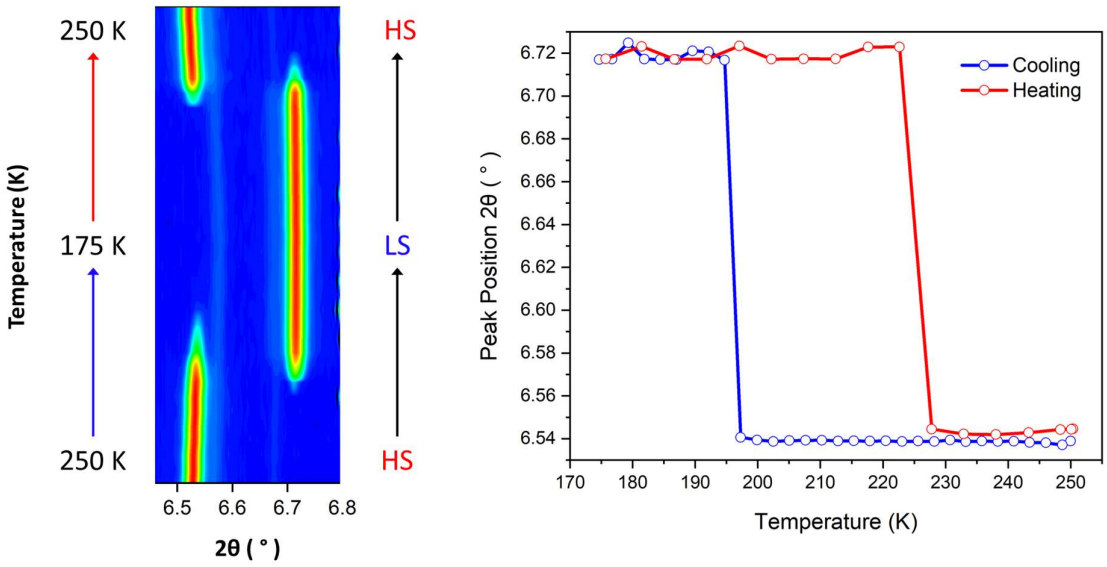

Figure S8. VT-PXRD data for **Pt(benpy)** showing (a) the evolution of a single Bragg peak (011) versus temperature (250 – 175 – 250 K) and (b) the quantitative temperature-dependence by peak fitting.

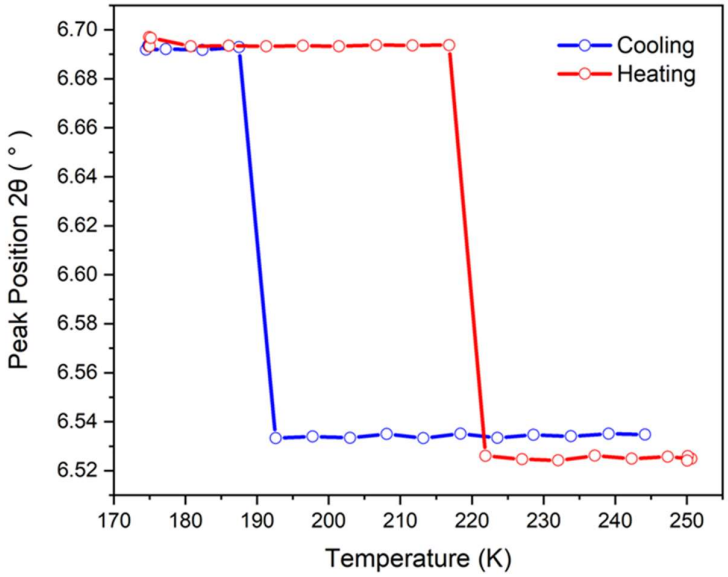

Figure S9. VT-PXRD data for **Pd(benpy)** (250 – 175 – 250 K) the quantitative temperature-dependence by peak fitting.

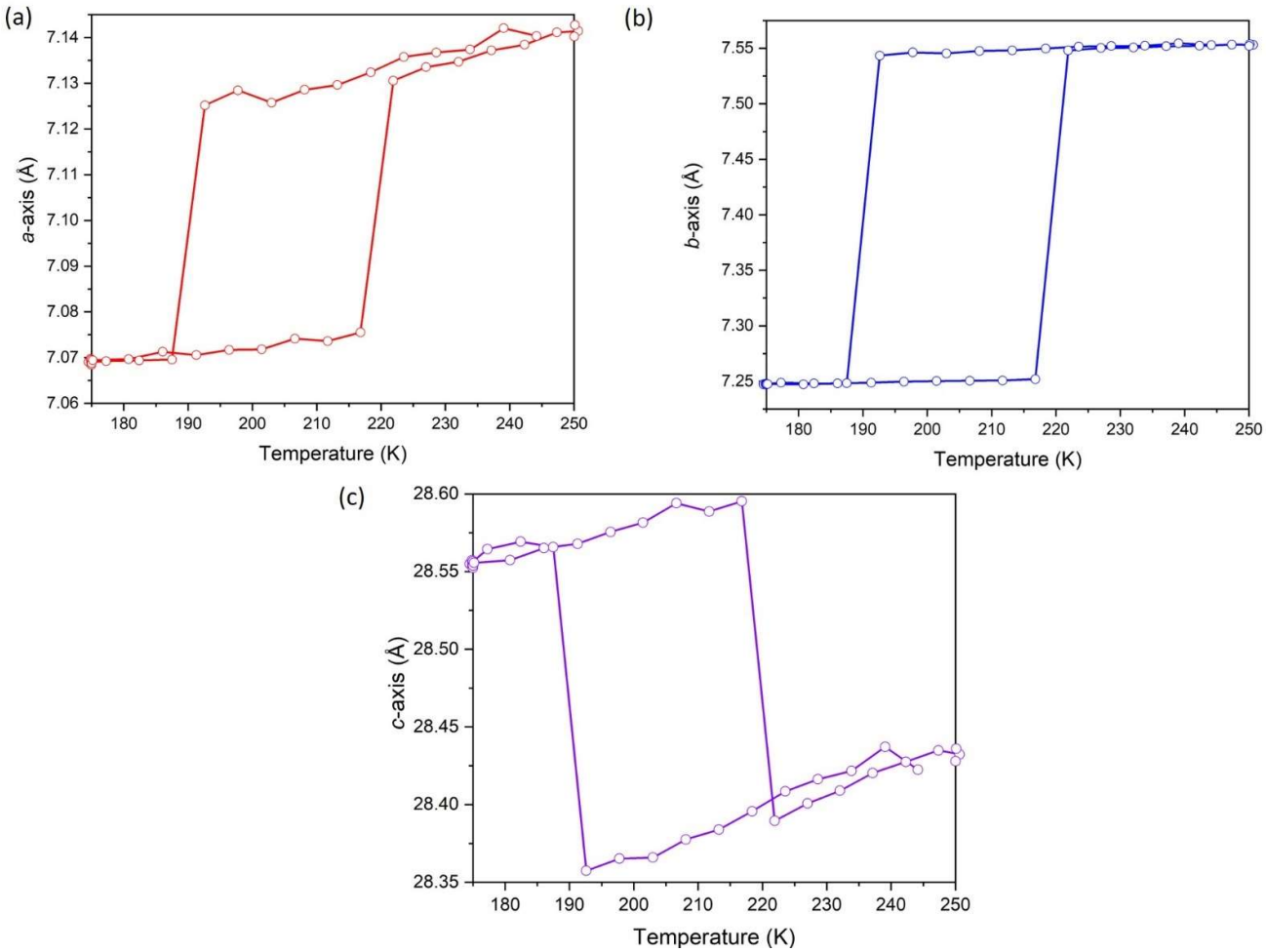

Figure S10. The temperature-dependence of the unit cell (a) *a*-axis, (b) *b*-axis and (c) *c*-axis extracted from Le Bail analysis of the individual PXRD patterns for **Pd(benpy)**.

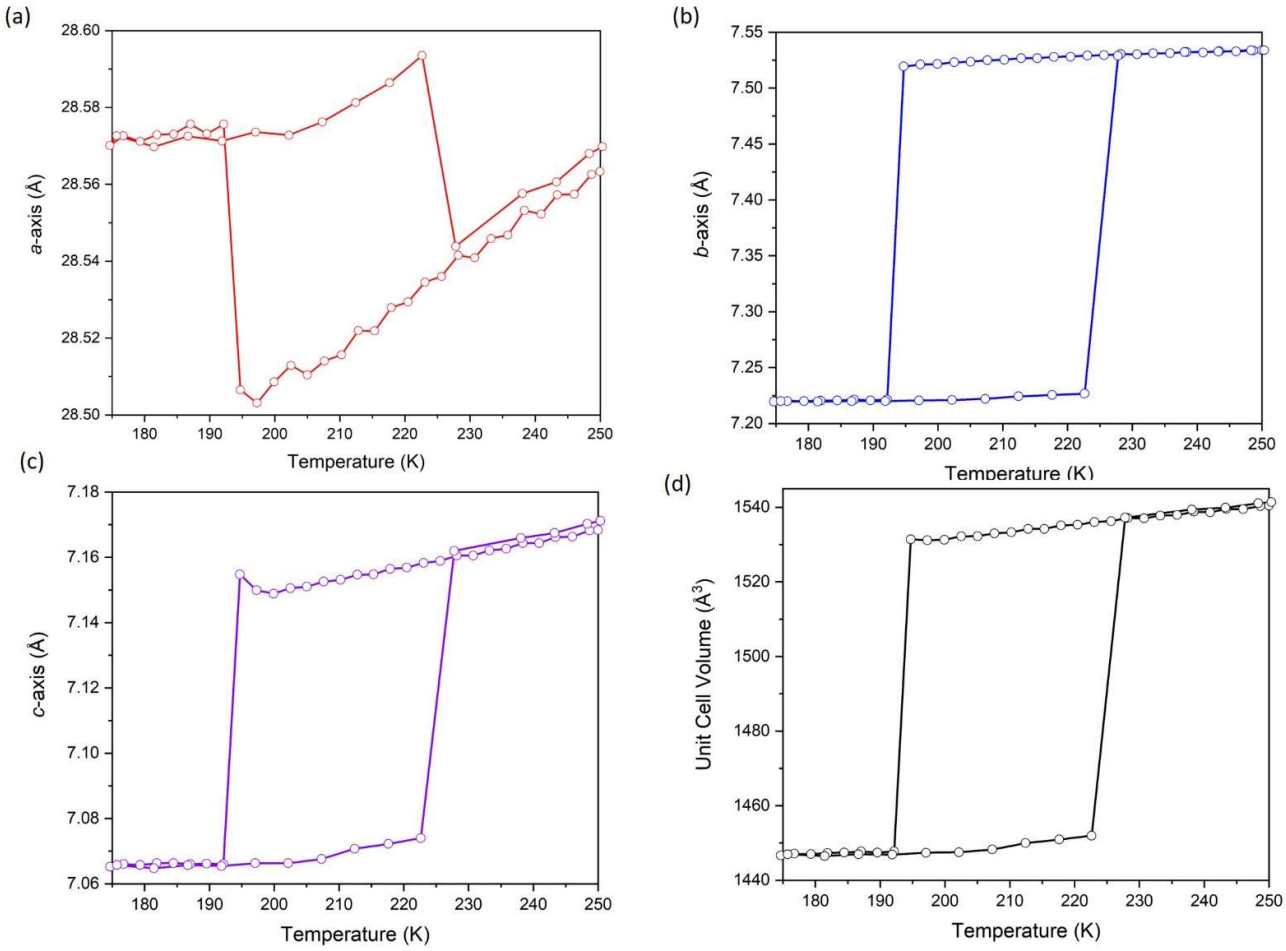

Figure S11. The temperature-dependence of the unit cell (a) *a*-axis, (b) *b*-axis, (c) *c*-axis and (d) volume extracted from Le Bail analysis of the individual PXRD patterns for **Pt(benpy)**.

S5. Variable Temperature Raman Spectroscopy

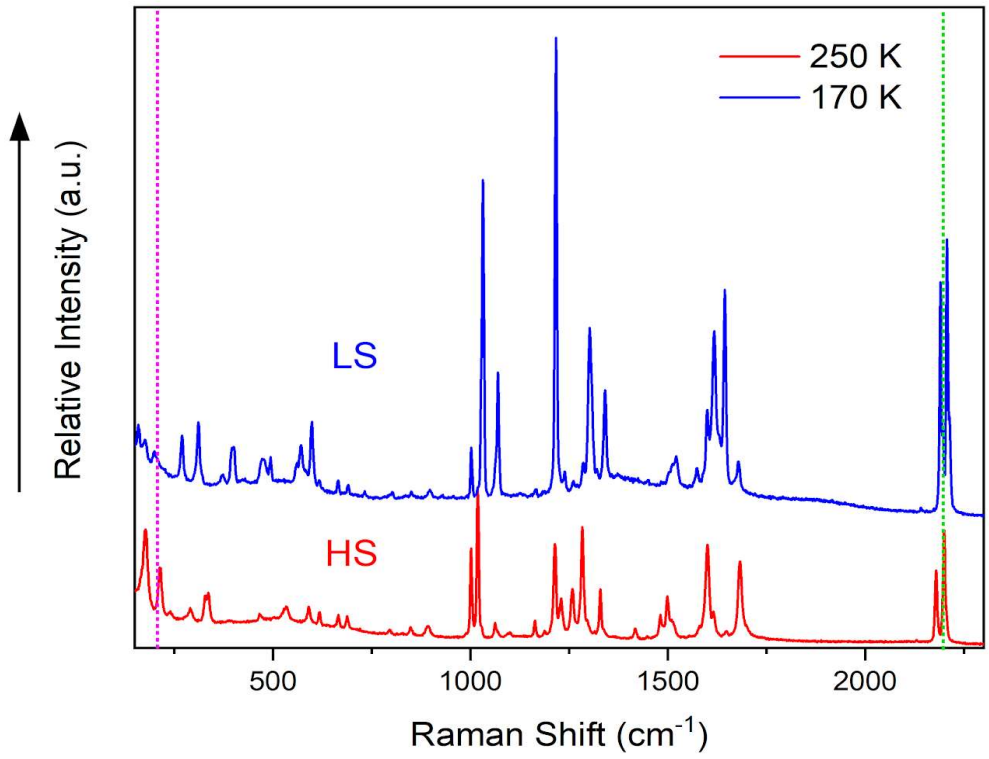

Figure S12. Variable temperature Raman spectroscopy data for **Pt(benpy)** at 250 and 170 K representative of the HS and LS states, respectively. The Fe-N (~225 cm^{-1}) and C≡N stretching (~2200 cm^{-1}) regions are indicated in pink and green, respectively.

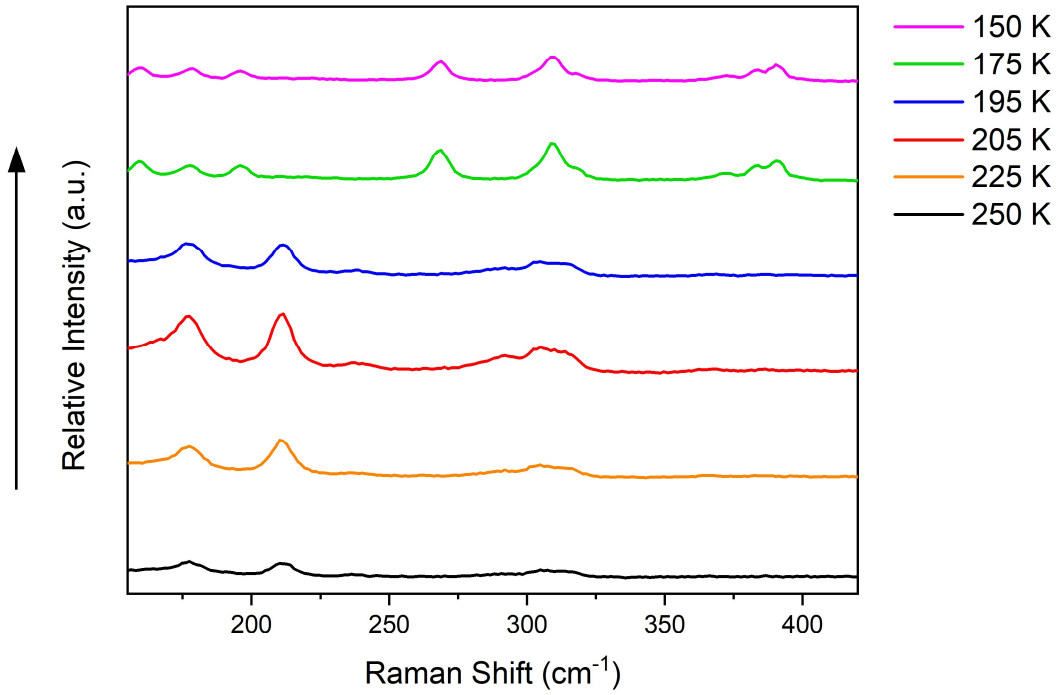

Figure S13. Variable temperature Raman spectroscopy data for **Pd(benpy)** in the 150 - 500 cm^{-1} range which encompasses the Fe-N and M-C stretching. The M-C stretching is typically in the 300 – 550 cm^{-1} range and and the Fe-N <300 cm^{-1}.

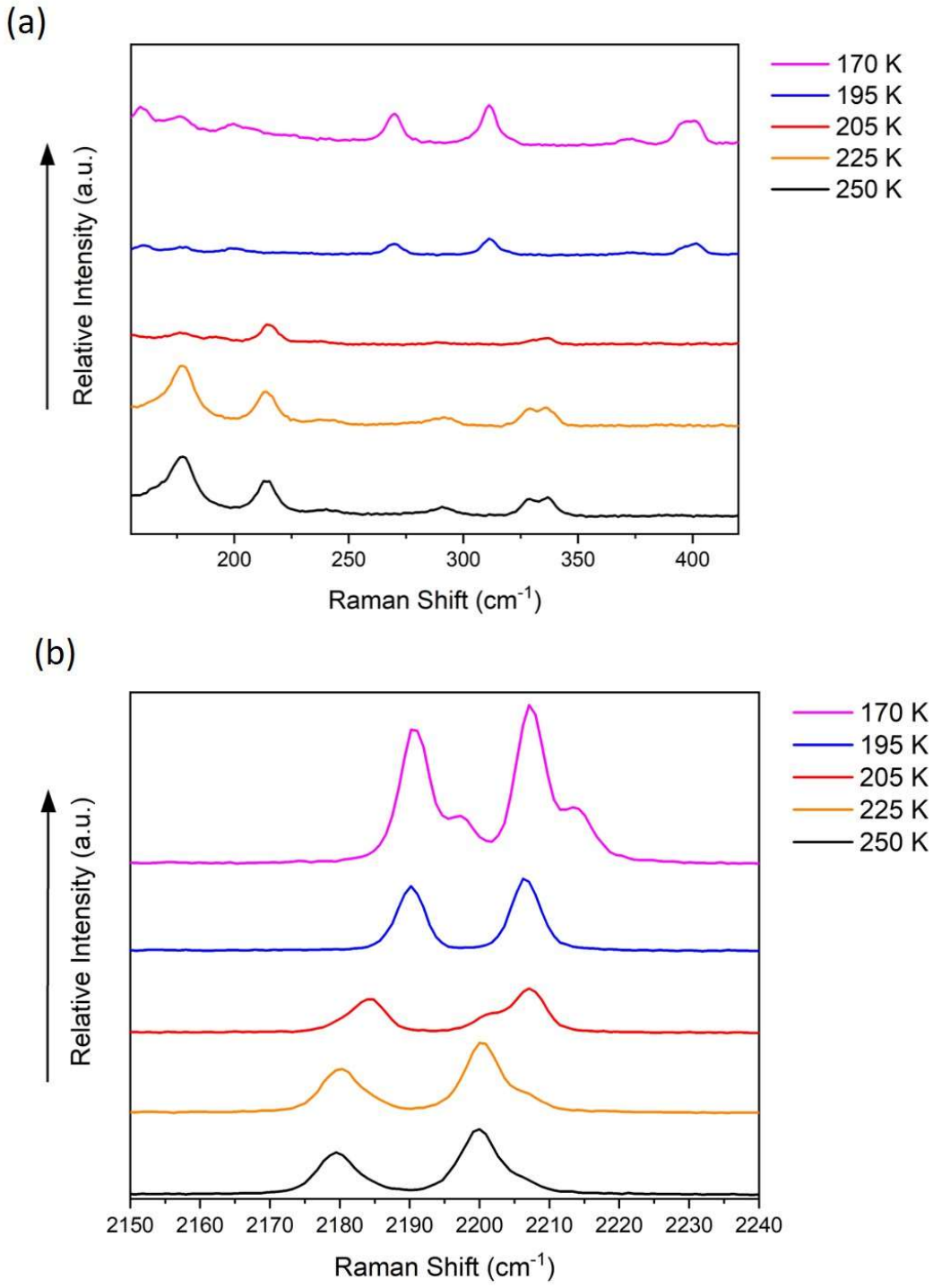

Figure S14. Variable temperature Raman spectroscopy data for **Pt(benpy)** showing the temperature-dependence of the (a) the Fe-N and (b) C≡N stretching frequencies over the spin-state change.

S6. Single crystal X-ray diffraction

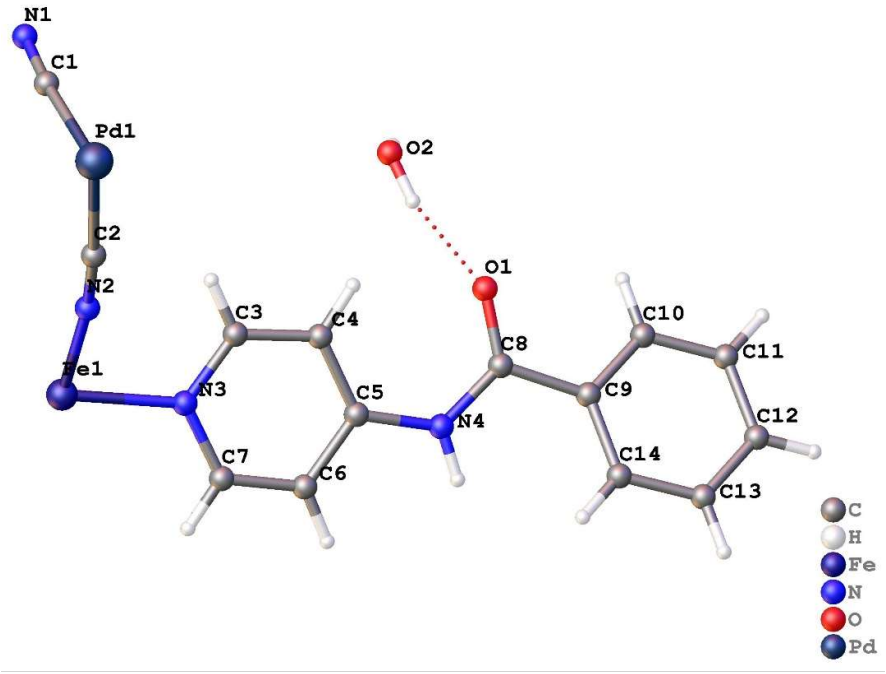

Figure S15. Thermal ellipsoid plot (50% probability) of the ASU of **Pd(benpy)** at 100 K.

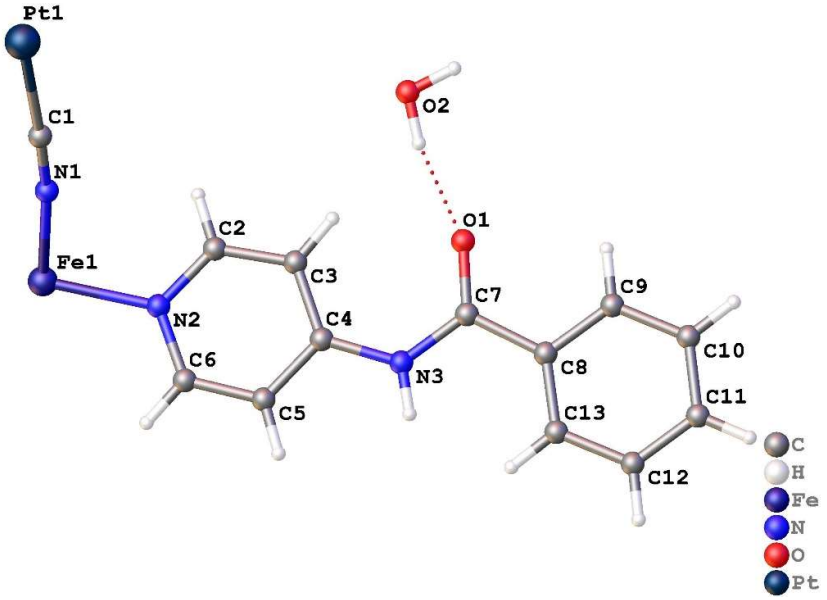

Figure S16. Thermal ellipsoid plot (50% probability) of the ASU of **Pt(benpy)** at 100 K.

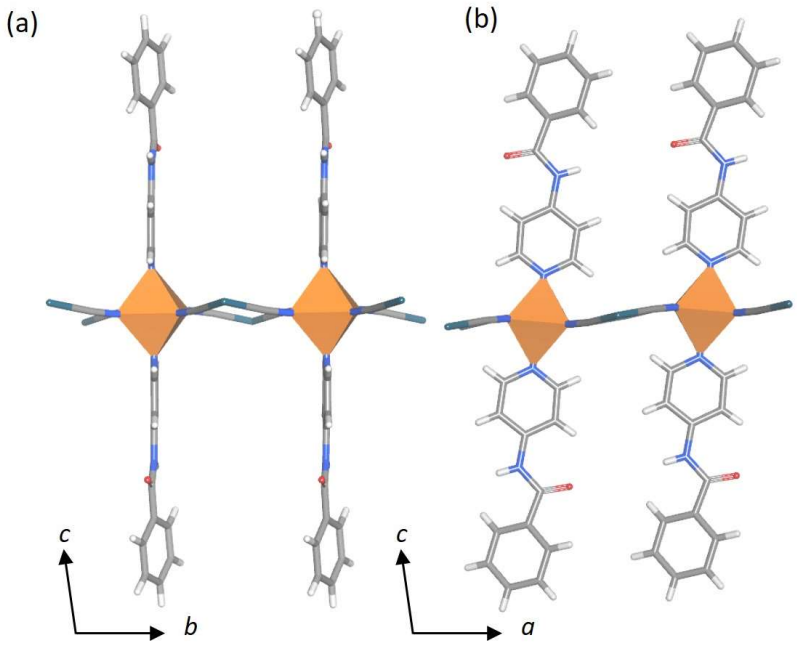

Figure S17. SCXRD structural representation of **Pd(benpy)** showing (a) torsional twist of the benpy ligands around the amide bond and (b) the relative positioning of the amide group between neighboring ligands and above and below the Hofmann layers.

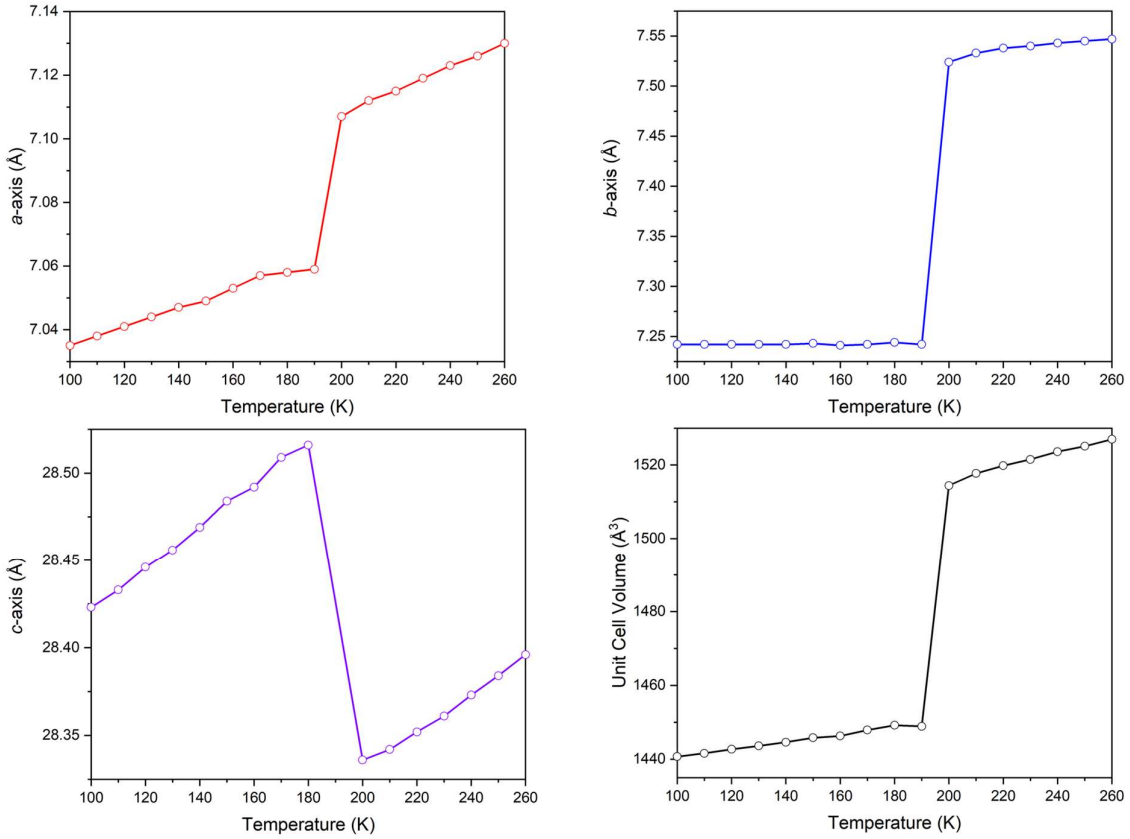

Figure S18. VT-SXTAL data for **Pd(benpy)** showing the unit cell (a) *a*-axis, (b) *b*-axis, (c) *c*-axis and (d) volume change with temperature over the range 250 – 100 K. Note: data were collected with cooling.

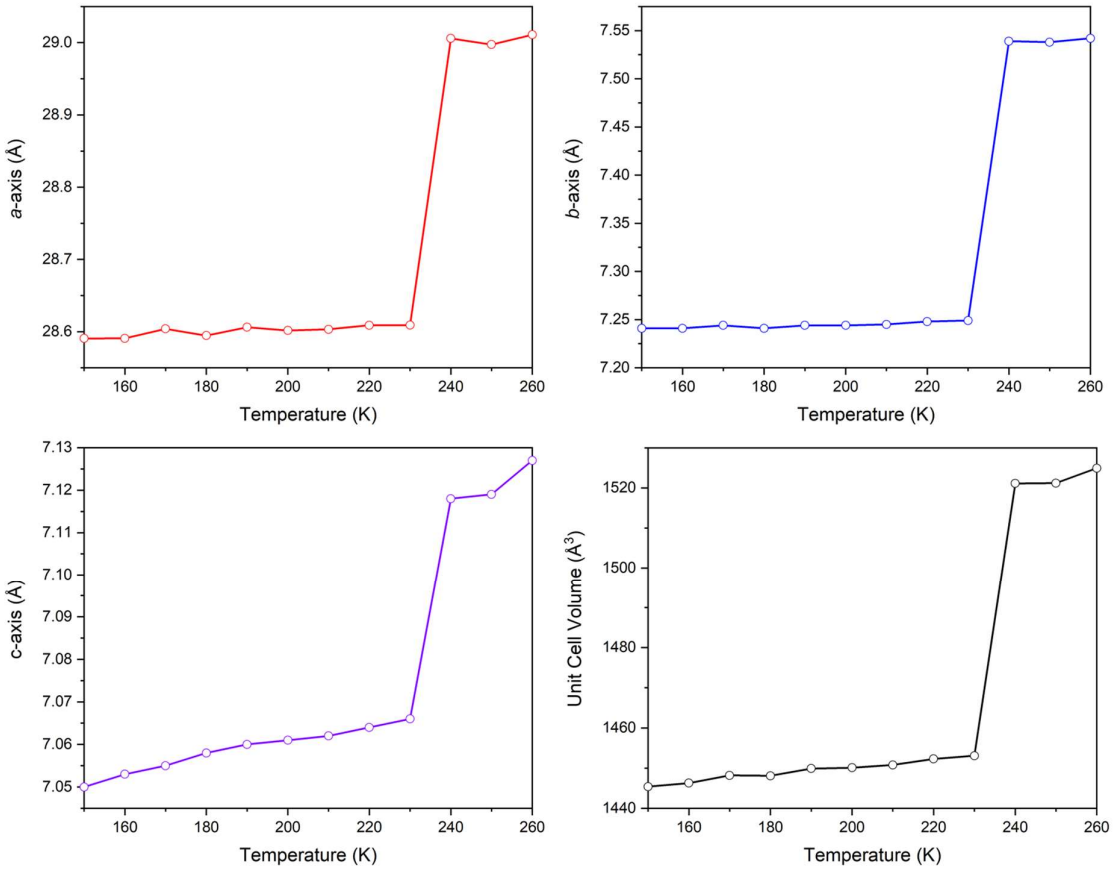

Figure S19. VT-SXTAL data for **Pt(benpy)** showing the unit cell (a) *a*-axis, (b) *b*-axis, (c) *c*-axis and (d) volume change with temperature over the range 100 – 250 K. Note: data were collected with warming.

Table S1. Representative crystallographic data and refinement details for **Pd(benpy)** and **Pt(benpy)** in the LS and HS states. Data for all other temperatures can be found in the CIF deposited in the CCDC.

Complex	$[Fe^{II}(benpy)_2Pd(CN)_4]\cdot 2H_2O$		$[Fe^{II}(benpy)_2Pt(CN)_4]\cdot 2H_2O$	
Formula / molar mass (g/mol)	$C_{28}H_{24}FeN_8O_4Pd$ / 698.82		$C_{28}H_{24}FeN_8O_4Pt$ / 787.48	
Temperature (K)	100	250	100	250
Space group	$P2_1/n$		$C2/m$	
a (Å)	7.035(14)	7.1260(14)	28.603(6)	29.013 (6)
b (Å)	7.2420(14)	7.5450(15)	7.2270(14)	7.5160 (15)
c (Å)	28.423(6)	28.384(6)	7.0530(14)	7.1550 (14)
β (°)	95.79(3)	92.03(3)	97.77(3)	101.13 (3)
Volume ($Å^3$)	1440.7(5)	1525.1(5)	1444.6(5)	1530.9 (6)
ρ_{calc} ($g\ cm^{-3}$)	1.611	1.522	1.893	1.708
μ (mm^{-1})	1.176	1.111	5.397	5.084
Data/restraints/parameters	3165 / 0 /196	3373 / 0 /196	1703 / 0 /130	1808 / 0 /130
Goodness-of-fit on F^2	1.062	1.062	1.065	1.056
Final R indexes [$I > 2\sigma(I)$]	$R_1 = 0.0287$ / $wR_2 = 0.0805$	$R_1 = 0.0225$/ $wR_2 = 0.0629$	$R_1 = 0.0321$ / $wR_2 = 0.0834$	$R_1 = 0.0556$ / $wR_2 = 0.1273$
Final R indexes R [all data]	$R_1 = 0.0365$ / $wR_2 = 0.0865$	$R_1 = 0.0281$ / $wR_2 = 0.0669$	$R_1 = 0.0321$ / $wR_2 = 0.0834$	$R_1 = 0.1009$/ $wR_2 = 0.1621$